J Neurosurg 106:175–179, 2007

Detection of the subthalamic nucleus in microelectrographic recordings in Parkinson disease using the high-frequency (> 500 Hz) neuronal background

Technical note

Peter Novak, M.D., Ph.D.,[1] Slawomir Daniluk, M.D.,[2] Samuel A. Ellias, M.D., Ph.D.,[1] and Jules M. Nazzaro, M.D.[2]

Departments of [1]Neurology and [2]Neurosurgery, Boston University School of Medicine, Boston, Massachusetts

✓Accurate and fast localization of the subthalamic nucleus (STN) during intraoperative electrophysiological monitoring can improve the outcome of deep brain stimulation surgery. The authors show a simple method of detecting the STN that is based on an analysis of the high-frequency (> 500 Hz) background (HFB) activity of neurons. The HFB reflects multiunit spiking activity close to the recording electrode, and its characteristic profile, which is higher in the STN than in neighboring structures, and facilitates delineation of both the dorsal and ventral STN borders.

Key Words • Parkinson disease • subthalamic nucleus • deep brain stimulation • microelectrode recording • high-frequency background

High-frequency stimulation of the STN is an effective treatment for Parkinson disease.[1] Stimulating electrodes are inserted via established stereotactic approaches for which STN coordinates are obtained from anatomical atlases and imaging studies. The target is usually refined using MER because of targeting errors related to inherent anatomical variability, the limited accuracy of imaging, and brain shift associated with opening of the dura mater and implantation of stereotactic hardware.[1,2,8,13,17,18] Microelectrode recording can improve the outcome of DBS surgery.[15]

A typical trajectory includes the thalamic nuclei, zona incerta, H2 field of Forel, STN, and SN. Characteristic neuronal patterns help differentiate the underlying structures during MER.[2,9,14,18,19] The STN is distinguished by increased neuronal background activity, increased spiking activity of the STN neurons, and kinesthetic responses.

The depth of the dorsal and ventral borders defines the STN width, which is a major determinant of the trajectory for implantation of the stimulating electrode.[16,19] The optimal trajectory captures the thickest part of the STN. Detection of the dorsal border is usually straightforward because there is an abrupt increase in neuronal activity as compared with that in the thalamus and zona incerta. Several factors can make electrophysiological determination of the ventral border more difficult: there are fewer kinesthetic neurons in the ventral STN, there can be islands of cells that have firing characteristics of both STN and SN cells, and quiet zones can be encountered as the electrode approaches the ventral border.

Electrophysiological determination of the STN borders by relying on the firing pattern can be difficult given that spike-sorting procedures are inherently time-consuming and subjective.[5] Several attempts have been made to eliminate the need to analyze the firing pattern. For example, Pesenti et al.[13] showed the usefulness of power spectrum calculations of the neuronal signals in estimating placement of the stimulating electrode within the STN without using the STN borders.

The relative increase in extracellular neuronal background noise is one of the electrophysiological criteria for STN localization. During DBS, surgeons usually monitor the neuronal background by viewing a display and listening to the neuronal signals via speakers.[19]

Extracellular neuronal background activity can be separated into two distinct types of signals according to their frequency characteristics.[11,20] The low-frequency background, also termed "local field potentials," consists of frequencies below 500 Hz and reflects the dendritic events. The HFB includes frequencies in the range of 500 to 3000 Hz and

Abbreviations used in this paper: ANOVA = analysis of variance; DBS = deep brain stimulation; HFB = high-frequency background; MER = microelectrode recording; MPTP = 1-methyl-4-phenyl-1,2,3,6-tetrahydropyridine; MR = magnetic resonance; SN = substantia nigra; STN = subthalamic nucleus.

measures the multiunit spiking activity. Given that many brain nuclei have a typical HFB magnitude,[4] the HFB profile may be useful as an electrophysiological marker for a particular structure. In the present study, we analyzed the HFB obtained from MER to determine whether it would aid in localization of the STN.

Materials and Methods

Patient Population

In this retrospective, single-center study, we analyzed data from the MERs of 15 patients (three women and 12 men) in whom idiopathic Parkinson disease[8] had been clinically diagnosed. Patient ages ranged from 48 to 74 years, the duration of disease was 8 to 23 years, and the mean modified Hoehn and Yahr score was 2.9 ± 0.52. The Unified Parkinson's Disease Rating Scale score in the off state was 63.1 ± 8.63 (total) and 37 ± 7.88 (Part III, Motor Examination). The institutional review board of the Boston University Medical Center approved the study.

Stereotactic Surgery

All dopaminergic medications were withheld from the patients for approximately 12 hours before surgery. All patients underwent bilateral DBS surgery, with 1 month between the first and second implantation. Thirty DBS leads were implanted. The right STN was targeted during the first surgery. The STN was directly visualized on 2-mm-thick axial T_2-weighted MR images acquired on a 1.5-tesla unit. The location of the left STN was obtained from the 2-mm-thick axial computed tomography sections that were fused with the preoperative MR images before the second surgery. The Cosman-Roberts-Wells stereotactic ring was placed parallel to the orbital-meatal line. The trajectory was projected from the frontal area to the bottom of the STN along a path just lateral to the ventricular system and through the anterior thalamus. Arc settings ranged from 60 to 70 degrees, and slide settings were 8 to 18 degrees; final settings were determined by the position of the stereotactic ring and underlying anatomy as seen on MR imaging. The exact trajectory was determined to avoid the sulci, ventricles, thalamostriate or other major veins, and internal capsule. The bur hole location in the frontal area was finally determined after calculating the individual trajectory as described previously. According to the Schaltenbrand and Wahren atlas,[17] the trajectory penetrates the following structures: anterior thalamus, zona incerta, H2 field of Forel, STN, and SN.

Intraoperative Electrophysiological Monitoring

Neural signals were recorded using a tungsten monopolar microelectrode (microTargeting electrode 10WVGGSE5-JN4; FHC) with impedance in the range of 0.2 to 0.4 MΩ measured at 1000 Hz (IMP-1, Bak Electronics) before the surgery. Intraoperatively, the impedance was repeatedly checked in each patient by using a LeadPoint system (Medtronic) to ensure that no major changes in impedance occurred. The electrode was advanced using a microdrive. The target was the bottom of the STN. The initial position of the microelectrode tip, referred to as 0 mm, was 15 mm above the target. The microelectrode was advanced in submillimeter steps, and 10-second segments of the extracellular signals were recorded. The electrophysiological criteria used to distinguish the STN included an increase in background activity, increase in neuronal firing (usual rate 35–50 Hz), and alteration in neural signals by passive movement of the contralateral limb. The criteria to distinguish the SN included a decreased neuronal background, high-frequency regular spiking, and an absence of kinesthetic responses. Neuronal activity was carefully monitored as described previously, and the dorsal and ventral STN borders were established. The STN width was the difference in the depth between the dorsal and ventral borders. Another track was undertaken if the STN width was less than 3.5 mm or if kinesthetic responses were absent. If the assignment of the ventral border was ambiguous—for example, because of quiet zones—another track was undertaken, and the track with the best kinesthetic responses and broadest STN width was chosen for final electrode implantation.

In each patient, the STN location was verified with intraoperative macrostimulation delivered via a DBS lead (model 3387; Medtronic) by inducing a contralateral improvement in the rigidity, tremor, or bradykinesia with stimulation up to 5 V without side effects. A mean of 1.6 tracks per operated side were obtained. No hemorrhages occurred during intraoperative electrophysiological monitoring.

Signal Processing

Microelectrode recordings were filtered using a 200- to 4500-Hz bandpass filter with a 6-dB-per-octave roll off, sampled at a rate of 14 kHz, converted to digital form with 16-bit resolution using a Leadpoint system (Medtronic), and stored in a computer for offline analysis.

Large spikes originating in proximity to a recording electrode obscure neuronal background activity; therefore, these spikes were removed from the neuronal signals by using threshold detection.[10] The threshold was set arbitrarily at ± 40 μV given that most of the well-differentiated spikes in our recordings had amplitudes greater than ± 60 μV. The spikes were replaced by zeros to preserve the equidistant sampling. Occasionally, we encountered high-frequency spike trains; these segments were excluded from analysis.

The power spectral density was calculated over the 10-second segments by using Welch's method[21] with a Fourier transform length of 6000 samples per segment weighted by Hamming window. In our study, the HFB was analyzed in the frequency domain and obtained by integrating the 500- to 2500-Hz band in the power spectral density. By this definition, the HFB equals the average power $\bar{P}$ of a neuronal signal over the 500- to 2000-Hz band $\bar{P}_{HFB}$. Figure 1 shows a schematic of the signal processing.

The STN borders based on the HFB analysis were obtained as follows: The dorsal border of the STN was defined as the point at which the $\bar{P}_{HFB}$ recording first exceeded 700. This value was chosen after preliminary statistical analysis of the HFB within the STN. Subsequently, the ventral border was defined as the last decrease in the $\bar{P}_{HFB}$ below 700 after having exceeded 700. Accordingly, the transient quiet zones, even with a $\bar{P}_{HFB}$ value below 700, were still considered to be a part of the STN. The signal processing software was written in Matlab (version 6.1; The MathWorks, Inc.).

Statistical Analysis

Only the recording of the trajectory that was chosen for

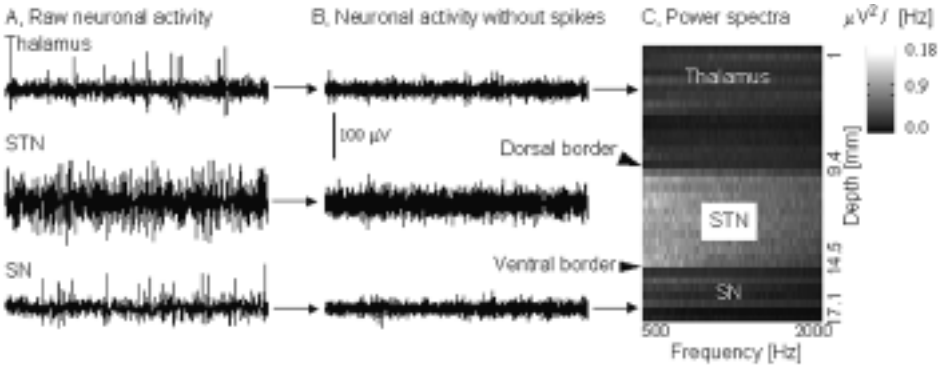

FIG. 1. Schematic demonstrating the processing of neuronal data. *Small arrows* show the flow of processing. Microelectrode recording traces (A) were obtained from the anterior thalamus (depth 4 mm), STN (depth 11.5 mm), and SN (depth 16.1 mm). Only a 0.25-second portion of the recordings is represented. Neuronal background traces (B) were obtained by removing large spikes from raw neuronal activity (A). High-frequency neuronal background was analyzed in the frequency domain by calculating spectral power densities (C) from the neuronal background. Each line in C represents a power spectral density at high frequencies (range 500–2000 Hz) calculated from a 10-second segment obtained at different electrode depths. The HFB that corresponds to a spectral power within the 500- to 2000-Hz range is elevated in the STN, with sharp changes in the spectral density at the dorsal and ventral borders, which are designated by *large arrowheads.*

the final electrode implantation was subjected to statistical analysis. We used 2 × 2 (borders × sides) ANOVA to compare the difference between the depths of the STN borders obtained using intraoperative electrophysiological monitoring and the depths determined using the HFB method. The overall difference in the means of $\bar{P}_{HFB}$ among the structures (thalamus/zona incerta, STN, and SN) was analyzed using 3 × 2 (structures × sides) ANOVA. The Tukey post-hoc test was applied for pairwise comparisons if the results of the ANOVA indicated overall significance. Statistical software (JMP version 5.1; JMP) was used for all statistical analyses.

Results

Figure 1 features a typical example of neuronal data from the thalamus, STN, and SN as recorded from a single microelectrode track. The corresponding HFB profile is shown in Fig. 2. An averaged profile of the HFB across all 30 recordings appears in Fig. 3. The HFB did not distinguish the anterior thalamus from the zona incerta; its magnitude was similar in both structures. In several patients, there was a noticeable decrease in the HFB just before entering the STN. The HFB abruptly increased as the electrode penetrated the dorsal border of the STN. The HFB varied within the STN but typically remained above the level of the thalamus/zona incerta. In four patients, there was a drop in the HFB as the electrode went deeper into the STN, but the HFB returned to the elevated level on further advancing of the electrode. Exit from the STN was associated with a sudden decrease in the HFB. The decrease was typically less steep compared with changes in the HFB across the dorsal border. The HFB in the SN remained at a lower level than in the STN.

Figure 4 shows an example of two successive HFBs obtained from the same patient. The first track missed the STN according to both intraoperative electrophysiological monitoring and HFB criteria. The second track fulfilled the electrophysiological criteria for the optimal STN localization; this track was chosen for DBS lead placement. In this track, the HFB was increased within the STN, and both dorsal and ventral borders could be easily distinguished.

All STN borders determined using HFB analysis were obtained automatically, according to the criteria defined in *Materials and Methods.* According to intraoperative electrophysiological monitoring, the mean depth of the STN dorsal border was 10.4 ± 0.91 mm on the right side and 10.7 ± 1.25 mm on the left. With HFB analysis, the mean dorsal border depth was 10.3 ± 0.80 mm on the right and 10.4 ± 1.27 mm on the left. Right and left ventral border depths were 14.8 ± 0.5 mm and 15.3 ± 1.46 mm, based on electrophysiological monitoring, and 14.9 ± 0.80 mm and 15.2 ± 1.53 mm, respectively, with HFB analysis. There was no significant difference (at the $p < 0.05$ level) in the

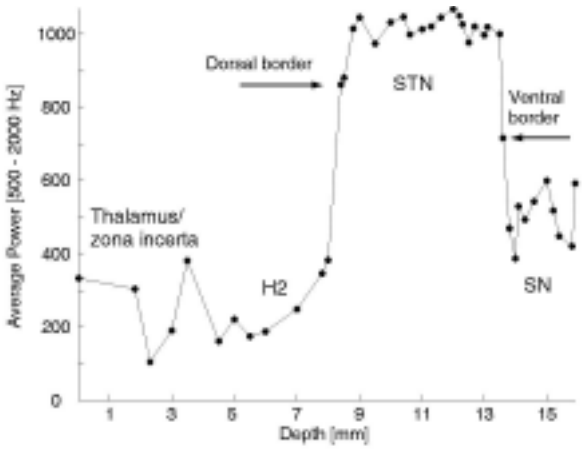

FIG. 2. Graph revealing a representative profile of HFB activity as a function of electrode depth. Each *circle* represents a mean HFB power ($\bar{P}_{HFB}$) obtained from a 10-second recording. *Arrows* indicate the STN borders. The dorsal border depth was 9.4 mm; the ventral border depth, 14.5 mm. The borders obtained using the HFB method were identical to those obtained during intraoperative electrophysiological monitoring. H2 = H2 field of Forel.

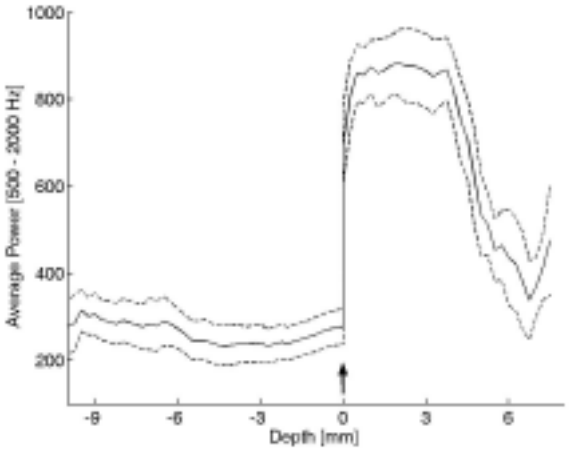

FIG. 3. Graph depicting the average HFB activity *(solid line)* and 95% confidence intervals *(dotted lines)* obtained from 30 neuronal intraoperative recordings. The mean HFB powers obtained from each patient were aligned at the dorsal STN border (*arrow,* depth 0 mm) and then averaged. The electrode trajectory starts on the left.

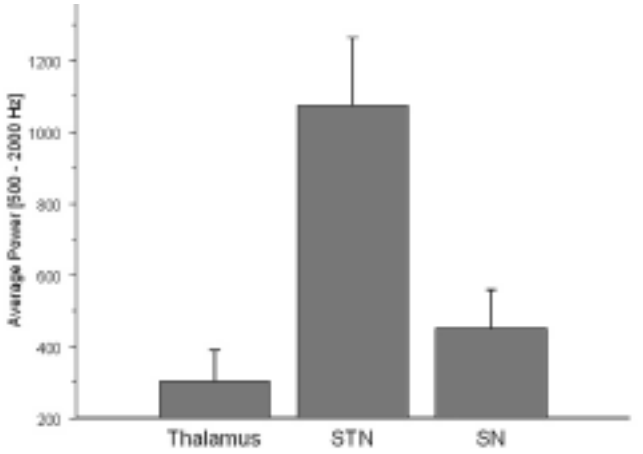

FIG. 5. Bar graph demonstrating the mean values and respective standard deviations of the high-frequency neuronal background activity obtained from the thalamus/zona incerta, STN, and SN.

estimation of borders, either dorsal or ventral, between the two methods. The left STN borders were deeper than those on the right, but the difference was not statistically significant. The mean STN widths obtained electrophysiologically and by HFB analysis were 4.78 ± 0.68 mm and 4.72 ± 0.68 mm, respectively, but the difference was not significant.

Results of an ANOVA showed a significant difference in the $\overline{P}_{HFB}$ among analyzed anatomical structures ($p < 0.0001$; Fig. 5). The $\overline{P}_{HFB}$ was higher in the STN ($p < 0.05$) than in either the anterior thalamus/zona incerta or the SN. For all structures, there was no significant difference in the $\overline{P}_{HFB}$ between the left and right sides.

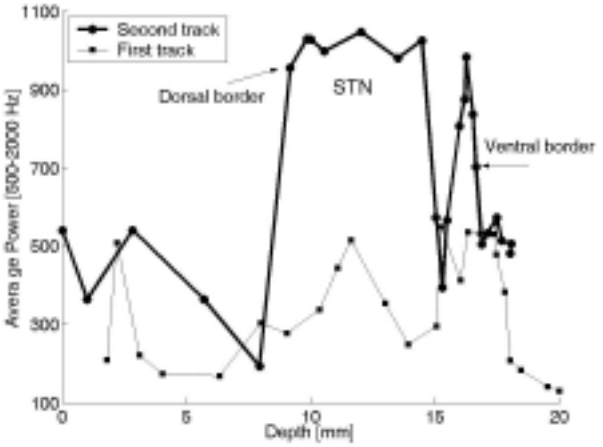

FIG. 4. Graph featuring examples of optimal and suboptimal tracks visualized by HFB activity. There is no elevation in the HFB activity within the depth of the STN on the first track, which missed the STN. Neuronal activity obtained from the second track, placed 2 mm medially with respect to the first track, has increased the HFB activity within the STN. There is also a quiet zone associated with a transient decrease in the HFB within the STN at a depth of 15 mm. In this patient, the dorsal border was assigned at an identical depth during both intraoperative electrophysiological monitoring and HFB analysis (9.17 mm). During electrophysiological monitoring, ventral border assessment was ambiguous, because there was a decrease in neuronal activity including both the spiking and neuronal background at a depth of 15 mm. Both spiking and neuronal background activity increased with further advancing of the electrode until a sustained decrease in neuronal activity was observed. According to the HFB criteria, the ventral border depth was at 16.6 mm. Each *circle* represents a mean HFB power ($\overline{P}_{HFB}$) obtained from a 10-second recording.

Discussion

In this study, we performed a quantitative analysis of the HFBs obtained during DBS surgery in patients with Parkinson disease. The HFB is higher in the STN than in the anterior thalamus, zona incerta, or SN. This finding confirms previous qualitative observations regarding the active neuronal background of the STN. Plotting the HFB as a function of the electrode depth enables easy visualization of the STN borders. There was good agreement between electrophysiological monitoring and HFB analysis in estimating the STN borders. The presented approach is fast and can be used on a real-time basis during DBS surgeries. In fact, HFB analysis of a 10-second segment takes a fraction of a second on a portable laptop powered by an Intel IV processor running at 1.2 GHz. Our results are consistent with previous observations suggesting that the HFB could be used as a guide for stereotactic electrode placement.[4] Nevertheless, the value of this approach remains to be established in a prospective study. Furthermore, although our study data suggest that estimating the STN borders with HFB analysis can be performed automatically without the need to analyze the firing pattern, the HFB analysis cannot replace intraoperative electrophysiological monitoring given that kinesthetic responses are necessary to confirm that the electrode is located in the sensorimotor part of the STN.

The HFB profile also exemplifies the inherent difficulties associated with the intraoperative electrophysiological monitoring. In four patients, there was a decrease in both neuronal spiking activity and neuronal background when the microelectrode was positioned close to the ventral STN border (Fig. 4). The decrease could correspond to the area

within the STN where the electrode encounters less active cells. When the electrode was advanced further, the spiking increased and the background activity returned to its elevated level, thus indicating that the monitored structure was still the STN. In these cases, a quantitative HFB profile could be helpful in determining the ventral STN border by removing the subjectivity in the assessment of the neuronal background level. The exact location of the ventral border is not merely an academic question given that the STN width, defined as the difference between the dorsal and ventral border depths, is used to determine the final placement of the stimulating electrode.[16,19]

High-frequency background activity reflects an aggregate of the spiking activity in the vicinity of the recording electrode.[11] Earlier study data[4] have shown that the HFB within the frequency range of 500 to 3000 Hz has a characteristic amplitude that differentiates specific brain regions. For example, the thalamic HFB is two to three times greater in amplitude than the HFB of the caudate nucleus, and it is four times greater in the red nucleus than in the SN. The amplitude of the HFB is proportional to the size of the cells at the recorded site and to the magnitude of extracellular spike potentials.[4,6] Interestingly, the HFB does not correlate with cell density.[4] The human STN contains large cells (25–50 μm[7,12]) that could generate the high amplitude HFB. In addition, the STN is hyperactive in Parkinson disease, and that can be another factor contributing to elevated HFB. This view is supported by experimental evidence utilizing the MPTP model of experimental parkinsonism. Exposure to MPTP induces a hyperactive STN that is accompanied by increased HFB in the STN in monkeys.[3] The HFB in the human STN affected by Parkinson disease could therefore reflect multiple-unit spiking activity arising from the large STN cells that are hyperactive due to the dopamine deficit.

Conclusions

The quantitative HFB analysis can be a useful adjunct to intraoperative MER in facilitating localization of the STN.

Disclosure

A provisional patent based on the method described in this study has been filed with the US Patent and Trademark Office. The patent is the property of Boston Medical Center Corporation.

Acknowledgment

Drs. Daniluk, Ellias, and Nazzaro contributed equally to this study.

References

1. Benabid AL: Deep brain stimulation for Parkinson's disease. **Curr Opin Neurobiol 13:**696–706, 2003
2. Benazzouz A, Breit S, Koudsie A, Pollak P, Krack P, Benadib AL: Intraoperative microrecordings of the subthalamic nucleus in Parkinson's disease. **Mov Disord 17 (3 Suppl):**S145–S149, 2002
3. Bezard E, Boraud T, Bioulac B, Gross CE: Involvement of the subthalamic nucleus in glutamatergic compensatory mechanisms. **Eur J Neurosci 11:**2167–2170, 1999
4. Buchwald JS, Grover FS: Amplitudes of background fast activity characteristic of specific brain sites. **J Neurophysiol 33:**148–159, 1970
5. Buzsaki G: Large-scale recording of neuronal ensembles. **Nat Neurosci 7:**446–451, 2004
6. Grover FS, Buchwald JS: Correlation of cell size with amplitude of background fast activity in specific brain nuclei. **J Neurophysiol 33:**160–171, 1970
7. Hardman CD, Henderson JM, Finkelstein DI, Horne MK, Paxinos G, Halliday GM: Comparison of the basal ganglia in rats, marmosets, macaques, baboons, and humans: volume and neuronal number for the output, internal relay, and striatal modulating nuclei. **J Comp Neurol 445:**238–255, 2002
8. Hughes AJ, Daniel SE, Kilford L, Lees AJ: Accuracy of clinical diagnosis of idiopathic Parkinson's disease: a clinico-pathological study of 100 cases. **J Neurol Neurosurg Psychiatry 55:**181–184, 1992
9. Hutchison WD, Allan RJ, Opitz H, Levy R, Dostrovsky JO, Lang AE, et al: Neurophysiological identification of the subthalamic nucleus in surgery for Parkinson's disease. **Ann Neurol 44:** 622–628, 1998
10. Lewicki MS: A review of methods for spike sorting: the detection and classification of neural action potentials. **Network 9:** R53–R78, 1998
11. Logothetis NK: The underpinning of the BOLD functional magnetic resonance imaging signal. **J Neurosci 23:**3963–3971, 2003
12. Parent A, Hazrati LN: Functional anatomy of the basal ganglia. II. The place of subthalamic nucleus and external pallidum in basal ganglia circuitry. **Brain Res Rev 20:**128–154, 1995
13. Pesenti A, Rohr M, Egidi M, Rampini P, Tamma F, Locatelli M, et al: The subthalamic nucleus in Parkinson's disease: power spectral density analysis of neural intraoperative signals. **Neurol Sci 24:**367–374, 2004
14. Pollak P, Krack P, Fraix V, Mendes A, Moro E, Chabardes S, et al: Intraoperative micro- and macrostimulation of the subthalamic nucleus in Parkinson's disease. **Mov Disord 17 (Suppl 3):** S155–S161, 2002
15. Priori A, Egidi M, Pesenti A, Rohr M, Rampini P, Locatelli M, et al: Do intraoperative microrecordings improve subthalamic nucleus targeting in stereotactic neurosurgery for Parkinson's disease? **J Neurosurg Sci 47:**56–60, 2003
16. Saint-Cyr JA, Hoque T, Pereira LCM, Dostrovsky JO, Hutchison WD, Mikulis DJ, et al: Localization of clinically effective stimulating electrodes in the human subthalamic nucleus on magnetic resonance imaging. **J Neurosurg 97:**1152–1166, 2002
17. Schaltenbrand G, Wahren W: **Atlas for Stereotaxy of the Human Brain.** Stuttgart: Georg Thieme, 1977
18. Starr PA: Placement of deep brain stimulators into the subthalamic nucleus or globus pallidus internus: technical approach. **Stereotact Funct Neurosurg 79:**118–145, 2002
19. Sterio D, Zonenshayn M, Mogilner AY, Rezai AR, Kiprovski K, Kelly PJ, et al: Neurophysiological refinement of subthalamic nucleus targeting. **Neurosurgery 50:**58–69, 2002
20. Super H, Roelfsema PR: Chronic multiunit recordings in behaving animals: advantages and limitations. **Prog Brain Res 147:** 263–282, 2005
21. Welch PD: The use of fast Fourier transform for the estimation of power spectra: a method based on time averaging over short, modified periodograms. **IEEE Trans Audio Electroacoust 15:** 70–73, 1967

Manuscript received October 24, 2005.
Accepted in final form June 26, 2006.
Address reprint requests to: Peter Novak, M.D., Ph.D., Department of Neurology, Boston Medical Center, 715 Albany Street, D315, Boston, Massachusetts 02118. email: peter.novak@bmc.org.